Egyptian Geophysical Society
EGS Journal, Vol. 16, No. 1, 135-144 (2018)

ASSESSMENT OF FRACTURE SYSTEMS AND THEIR CONTRIBUTION IN THE GROUNDWATER OCCURRENCES IN CARBONATE ROCKS USING GEOELECTRIC TECHNIQUES IN El-HASSANA AREA, NORTH SINAI, EGYPT (CASE STUDY)

H.H. MAHMOUD

Geophysical Exploration Department, Desert Research Center, Cairo, Egypt.

تقييم نظم التشقق ومساهمتها في تواجد المياه الجوفية في الصخور الجيرية باستخدام التقنيات الجيوكهربية بمنطقة الحسنة – شمال سيناء – مصر (دراسة حالة)

الخلاصة: تمثل المياه الجوفية بمنطقة الحسنة المصدر الرئيسي لامدادات المياه التي تستخدم لجميع الاغراض. وأدي الطلب المتزايد علي المياه ومحدودية مواردها الطبيعية في هذه المنطقة القاحلة الي زيادة الحاجة الي استكشاف مصادر جديدة للمياه الجوفية. وأوضح الحفر العشوائي لابار جديدة في الصخور الكربوناتية لعصر الكريتاوى العلوي، أن بعض هذه الآبار منتجة والبعض الآخر جافة. وتوضح هذه الظاهرة أن تواجدات المياه الجوفية تعتمد أساسا علي تواجد نطاق تشقق بالصخور والتي تحتاج الي تقنيات جيوفيزيقية خاصة. تم استخدام المقاومة النوعية التصويرية والتي تشمل كلا من التقنيات ثنائية وثلاثية الأبعاد بشكل فعال لتحديد أنظمة التشقق في الصخور الكربوناتية الضحلة. وقد أجريت قياسات باستخدام ترتيب فينر للأقطاب الموجه في الموقع المحدد بناء علي نتائج المسح الثنائي والثلاثي الأبعاد. واتضح من التفسير التخطيطي لبيانات توزيع فينر للاقطاب أن المقاومة النوعية المقاسة تتغير بتغير اتجاه توزيع الأقطاب وذلك لكل المسافات البينية بين الأقطاب ووجد أن الاتجاه السائد للتشقق هو ٢٢,٥ درجة شمالا. ووجد أن التباين الراسي المؤثر المحسوب يتغير مع العمق نتيجة للتغير الطفيف في اتجاه التشقق او التغيرات في كثافة التشقق أو كلاهما معاً. وقد تم تأكيد هذه النتائج باستخدام توزيع الاقطاب الرباعي الموجه.

ABSTRACT: *Groundwater in El Hassana area represents the main source of water supply which in used for all purposes. The increasing demand on water and the limitation of its resources in this arid region increases the need to explore new groundwater resources. Random drilling of new wells in the Upper Cretaceous carbonate rocks show that, some of these wells were productive and some others were dry. This phenomenon exhibits that the groundwater occurrence depends mainly on the presence of a fracture zone which needs special geophysical techniques. Electric Resistivity Tomography including both 2-D and 3-D techniques were used effectively for delineating the fracture systems in shallow carbonate rocks. Azimuthal collinear Wenner array was conducted at a selected site based on the obtained results from both 2-D and 3-D surveys. Graphical interpretation of the Wenner array data indicated that the measured apparent resistivity changed with the orientation of the array for all a-spacing and the dominant fracture strike is found to be oriented at N 22.5 degrees. The calculated effective vertical anisotropy is found to be varied with depth due to slight variations in fracture strike and/or variations in fracture density. Results from the collinear Wenner array data are supported by azimuthal square array which the graphical interpretation coincides with that obtained from Wenner array.*

1. INTRODUCTION

The study area lies in the northern part of central Sinai at El Hassana City, it is bounded by latitudes 30o 27’ 34’’ and 30o 27’ 50’’ N and longitudes 33o 47’ 4’’ and 33o 47’ 20’’ E (Fig. 1). El Hassana area is located 75 km to the south of El Arish City; it lies in the great arid belt of Egypt. It is characterized by hot, long summer and mild, short winter periods with relatively low precipitation and high evaporation. Annual precipitation varies strongly over Sinai Peninsula, where it ranges from 10 mm/year at the southeastern part to more than 200 mm/year at the northeastern part. The study area is located in the zone of average annual rainfall of about 20-50 mm/year (Abou Rayan *et al.* 2001). Precipitation represents the main source of shallow groundwater recharge in the study area through fissures and fractures during heavy rains and torrents.

Groundwater in El Hassana area and its vicinities in the central Sinai has a special significance, where it represents the unique source of water supply in this arid region. This area suffers from lack of water supplies due to increase in water demands and limitation of groundwater resources. Water supplies are considered as one of the most critical factors in sustainable developments in this arid region. The local inhabitants depend mainly on the groundwater for drinking, domestic, livestock and irrigation purposes. Therefore the increasing demand on water in this arid region needs more exploration activities for new groundwater resources. The groundwater in El Hassana area occurs in fractured carbonate section. Some wells taped groundwater and some others were founded to be dry because it failed to catch the fracture zone. This phenomenon exhibits that the presence of groundwater is related to presence of fracture zone. So, the aim of the present work is to delineate the fracture zones for groundwater supply in shallow carbonate rocks by using integrated geoelectric resistivity techniques.

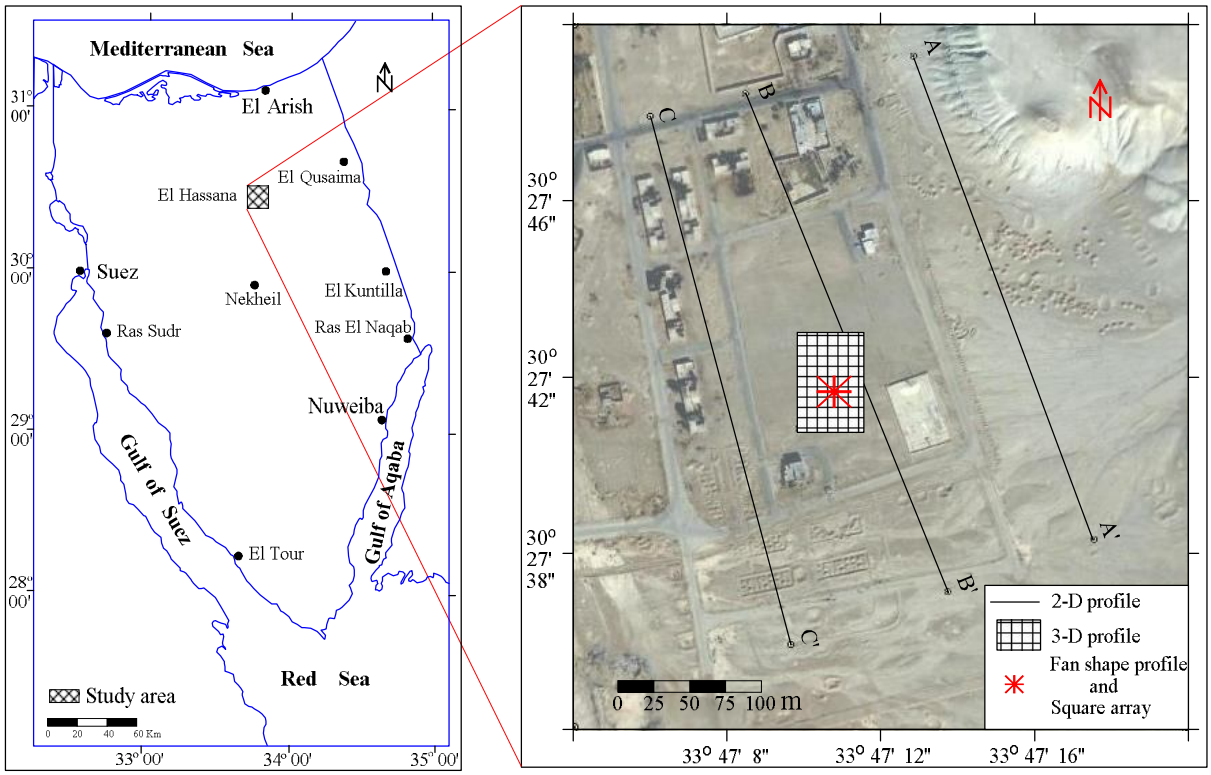

Fig. 1: Location map of the study area.

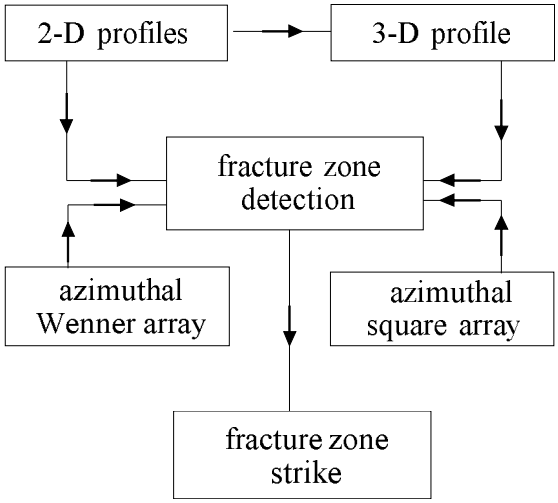

Fig. 2: Flow chart of field data acquisition.

To achieve the main target of this work, Electrical Resistivity Tomography (ERT), including both two dimensional resistivity imaging technique (2-D) and three dimensional resistivity imaging technique (3-D), were applied to accurately detect the fractured zone in massive carbonate rocks. Also, both azimuthal Wenner and square arrays were carried out to determine the fracture zone for water supply, fracture orientation and its effective vertical anisotropy (Fig. 2). The integration between these techniques can give more accurate results and reduce the ambiguity during interpretation.

2. GEOMORPHOLOGIC, GEOLOGIC AND HYDROGEOLOGIC SETTINGS

Geomorphologic setting of central Sinai was the subject of many studies, as the works of Shata (1960), Hammad (1980), El Ghazawi (1989), El Shamy (1992) and Hassanin (1997). According to Hassanin (1997) the investigated area is located in the hydrographic basins unit (inland drainage system). Wadi El Hassana is an elliptical basin, where its headwaters originated from the foot slopes of Gebel Yelleq and Gebel El Minshera. Its upstream channel extends in northeast direction for about 20 km and then turns to north northeast direction

for about 16 km and drain finally in the depression to the north of El Hassana City. This wadi is bounded by low cliffs from chalk, calcareous shale, dolomitic limestone with thin flint bands and occasional basaltic intrusions.

Upper Cretaceous (Senonian) rocks are exposed in El Hassana area overlying the Turonian Wata Formation (limestone and dolomite). Ghorab (1961) subdivided Senonian rocks of central Sinai into two formations. The lower one (Matulla Formation) belongs to Lower Senonian age. This formation is exposed south of El Hassana area and it attains a thickness of about 135m. It is composed of yellow fossilifereous marl and marly limestone with weathered flint bands of nodular appearance. Whereas, the upper formation (Suder Chalk) belongs to Upper Senonian age and follows conformably Matulla Formation having 160m thick. This formation composed of white massive chalk superficially weathered, with siliceous concretions and abundant filled cracks with crystalline calcite. The upper surface of the Suder Chalk is generally covered by recent gravels and alluvium deposits. The Campanaian – Maastrichtian Sudr Chalk of Gabal El Bruk, which is located to the south of the study area, is subdivided into two members, the lower Markha Member and the upper Abu Zenima Member (Issawi et al. 2009; El Beialy *et al.* 2010; Hassan and Abouelresh, 2013).

The structural elements of Sinai Peninsula were discussed in many works such as, Shata (1956), El Shazly et al. (1980), Moustafa and Khalil (1989) and Rabeh and Miranda (2007). According to these studies, the area under consideration is located in the fractured or shear zone. It extends in a northeast-southwest direction; this zone is influenced by a conjugate set of faults with NE and NW trends. The folds belong to this zone are asymmetrical anticlines oriented in NE-SW direction.

Hydrogeologically, the Upper Cretaceous carbonate rocks (interbedded limestone, chalk, dolomite and shale) are detected as water bearing formation at El Hassana area. This aquifer is tapped at shallow depths and its groundwater quality is brackish water (4787ppm); a small desalination unit depends on the groundwater extracted from El Hassana well was constructed to save water supplies in the study area. The storativity of this aquifer is low (0.035) while its transmissivity is moderately high (1840 m^2/day), this can be attributed to the lateral variation of the physical properties of the water bearing formation and the intricate fractures system, (Hassanin 1997).

Some geophysical studies were carried out in the study area and its vicinities along central Sinai with different purposes, from which the works of JICA (1992), Massoud (2005), Rabeh and Miranda (2007) and Sultan et al. (2015). These studies concluded that the deep aquifer (Nubian sandstone) in central Sinai is dissected by different structural elements of NE-SW and NW-SE trends. Al Abaseiry (2003) used Vertical Electrical Soundings to evaluate the groundwater potentiality in the area between El Qusaima and El Hassana, he concluded that the groundwater is present in carbonate rocks, and it is affected to large extend by fissures and fractures.

Rabeh and Miranda (2007) studied the subsurface structures of El Hassana area by using gravity and magnetic methods, they concluded that most prevailed tectonics in El Hassana area are trending at N 35^o-65^o E direction which related to the Syrian Arc Tectonic System direction. From these studies, it is clear that the shallow carbonate aquifer depends on the presence of fracture and its amounts; and the trend of the dominant structure is at NE direction.

3. DATA ACQUISITION AND PROCESSING

3.1. Two dimensional resistivity imaging:

Two dimensional resistivity imaging technique (2-D) was widely used to study groundwater occurrences in karstified/fractured limestone aquifers because the huge contrast in resistivities between the saturated fractured zone and its surrounding from the compact rocks. (Ioannis et al. 2002; Yadav and Singh 2007; Tanguy et al. 2011; Metwaly and Al Fouzan 2013; Tassy et al. 2014 and Mahmoud et al. 2015).

Three parallel 2-D resistivity imaging profiles (A-A', B-B' and C-C') were carried out in the study area to determine the fractured zone in carbonate rocks (Fig. 1). These profiles take nearly NNW-SSE direction perpendicular to the expected fractures directions that obtained from field observations and previous works. Field measurements of these 2-D resistivity profiles were made by applying Wenner alpha configuration using ABEM LUND imaging system (Terrameter SAS 1000, electrode selector ES 10-64, and multi conductor cables). Wenner array is characterized by its high signal strength and better signal to noise ratio and also it has a good vertical resolution. Field survey technique was carried out with a system where 61-steel electrodes are arranged along a line with 6m constant electrode spacing (a-spacing) at the same datum points and increasing this space by a multiply factor (2, 3, 4, etc….) to increase depth of investigation (Fig. 3), the total length of each profile is 360 m. RES2DINV software (GEOTOMO 2010) was used to invert the measured apparent resistivity data into a 2-D resistivity imaging model. This model demonstrates the low resistivity anomalies (karst or fractures saturated by groundwater) in the high resistivity background (compact carbonate rocks). Based on the steps of this software, a forward modeling subroutine (finite-difference method) is used to calculate the apparent resistivity values, and a non-linear least-squares optimization technique is used for the inversion routine (deGroot-Hedlin and Constable 1990; Loke and Barker 1996a). The 2-D model used by this program divides the subsurface into a number of rectangular blocks. The purpose of this program is to determine the resistivity of the rectangular blocks that will produce an apparent resistivity pseudosection that agrees with the actual measurements.

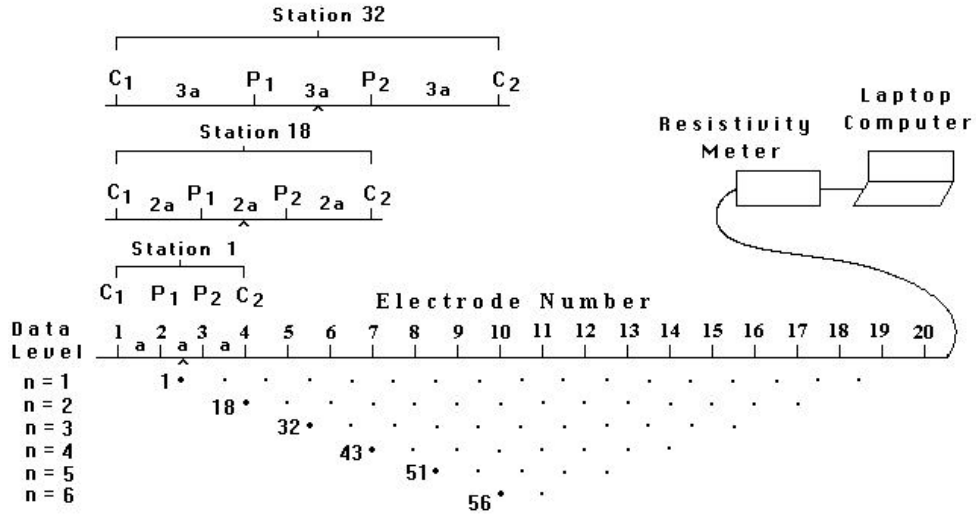

Fig. 3: Arrangement of electrodes for 2-D resistivity imaging survey (GEOTOMO, 2010).

Particularly for large resistivity contrasts, such as in this case, the mesh grid size was selected to be 4-nodes per electrode spacing and using finer mesh in the vertical direction to obtain more accurate calculated apparent resistivity values. The difference between the calculated and measured apparent resistivity values is given by the root-mean-squared (RMS) error.

3.2. Three dimensional resistivity imaging:

Based on the results that are obtained from the 2-D resistivity models, one 3-D resistivity imaging survey was carried out over the localized 2-D anomaly to accurately determine the characterization of this anomaly. Field measurements were done by applying pole-pole array.

The electrodes for such a survey (60-steel electrodes) are arranged in a uniform rectangular grid (10 electrodes in X-direction and 6 electrodes in Y-direction) with a constant spacing (7 m) between the electrodes in both X-direction and Y-direction. Cross-diagonal sequence technique was used to acquire the field data (Fig. 4). RES3DINV software (GEOTOMO 2010) was used to automatically determine a 3-D resistivity model for the subsurface (White et al. 2001). Data inversion using the Robust or blocky constraint (Loke et al. 2003) that is less sensitivity to noisy; it tends to produce models with regions of more uniform resistivity values with sharper boundaries. It divided the subsurface into a number of small rectangular prisms and attempts to determine the resistivity values of the prisms to minimize the difference between the calculated and observed apparent resistivity values; the widths of the rectangular blocks are equal to the unit electrode spacing in the X- and Y- directions. Forward modeling settings used finite-difference method to calculate the apparent resistivity values; the finite-difference grid with three nodes between adjacent

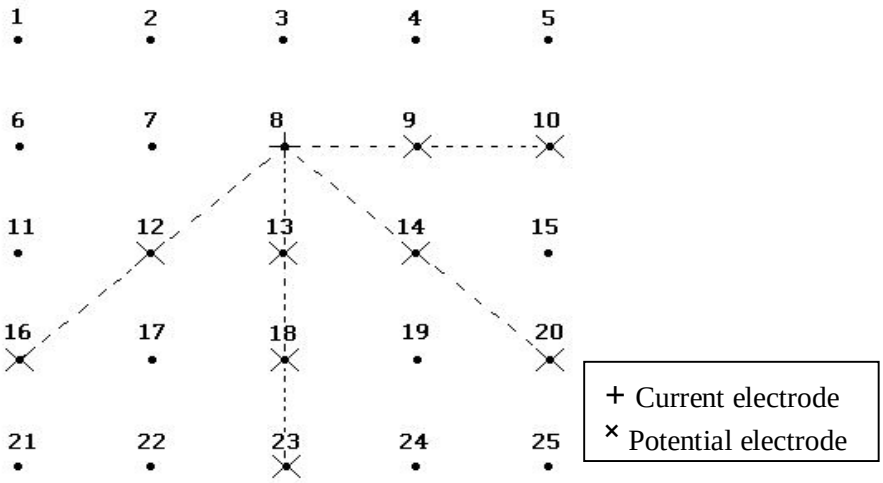

Fig. 4: Cross diagonal technique for 3-D resistivity imaging survey (GEOTOMO, 2010).

electrodes was used for more accuracy. A measure of the difference between the calculated and measured apparent resistivity values is given by the root-mean-squared (RMS) error.

3.3. Azimuthal Wenner array:

Direct current (DC) resistivity methods including both azimuthal collinear arrays and square array have the ability to detect bedrock fractures in massive rocks; they can provide directional information about resistivity variations. Collinear arrays including Wenner and Schlumberger arrays have been utilized successfully to detect bedrock fractures, where they are rotated about the array center point to measure azimuthal variation in the apparent resistivity (Taylor and Fleming 1988; Lieblich et al. 1991; Ritzi and Andolsek 1992). The azimthal Wenner array was conducted at the selected site based on the results that obtained from both 2-D and 3-D surveys to detect productive fracture zone in the carbonate rocks for groundwater supplies; it provides information about fracture strike and its anisotropy. It is carried out by applying Wenner array with different electrode spacing (a=40, 60, 80, 100 and 120m). The utilized configuration was rotated every 22.5 degrees about the central point of the array at the same a-spacing to measure the azimuthal variations in the apparent resistivity at the same depth.

Graphically, the apparent resistivity for Wenner array is plotted against the azimuth of that measurement; the direction of the maximum apparent resistivity for the collinear array is founded to be parallel to the fracture strike (Habberjam, 1972). The ratio of the apparent resistivity measured parallel to the fracture strike (ρ_{al}) to the apparent resistivity measured perpendicular to fracture strike (ρ_{at}) is called the apparent anisotropy (λ_a) and is given by the equation 1 (Darboux-Afouda and Louis, 1989).

$$\lambda_a = \rho_{al}/\rho_{at} = N \quad (1)$$

where N = effective vertical anisotropy

3.4. Azimuthal square array:

The results obtained from Wenner array was supported by applying square array. Square array method is more sensitive to a given rock anisotropy than the more commonly used collinear arrays, it requires about 65% less land area than the equivalent collinear arrays (Habberjam, 1972). This array was used to detect productive fracture zone in crystalline rocks (Darboux-Afouda and Louis 1989; Sehli 1990 and Lane *et al.* 1995). In this work, the measurement location is assigned to the center point of the square and the array size (A) is the length of the side of the square. Multiple square array data are collected using three A-spacing which are 53.3m, 80.0m and 106.7m which are equivalent to 40.0m, 60.0m and 80.0m a-spacing of Wenner array. The square was rotated every 22.5 degrees about the central point of the square at the same A-spacing. For each square, three measurements are taken, two perpendicular measurements alpha (α) and beta (β), and one diagonal measurement gamma (γ). Alpha and beta measurements give information on resistivity variations in the subsurface where gamma measurement serves as a check on the accuracy of alpha and beta measurements. The direction of the alpha and beta measurements is that of a line connecting the current electrodes (Fig. 5). The apparent resistivity can be calculated from equation 2 (Habberjam and Watkins 1967)

$$\rho_a = (2\pi A/2-\sqrt{2}) * \Delta V/I \quad (2)$$

where:

A = length of square, in meters

ΔV = potential difference, in volts

I = current, in amperes

The square resistivity measurements are reduced to a single measurement (ρ_m) by using equation 3 (Habberjam and Watkins 1967)

$$\rho_m = \sqrt{(\rho_{a\alpha})(\rho_{a\beta})} \quad (3)$$

where:

$\rho_{a\alpha}$ = calculated apparent resistivity using alpha configuration

$\rho_{a\beta}$ = calculated apparent resistivity using beta configuration

In this work, multiple square array data are collected to provide sufficient data for graphical display and interpretation of the individual square array data

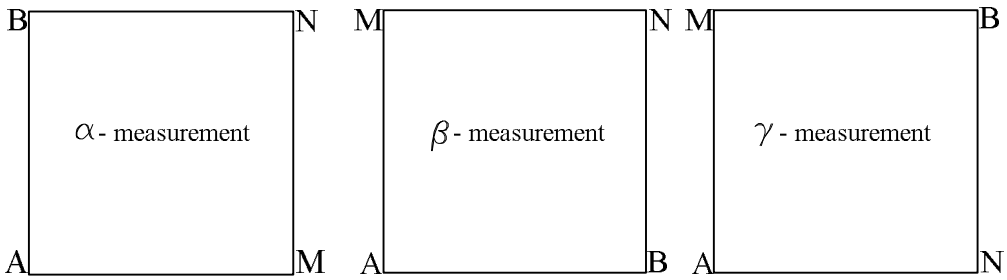

A and B are current electrodes M and N are potential electrodes

Fig. 5: Electrode positions of the different square array measurements.

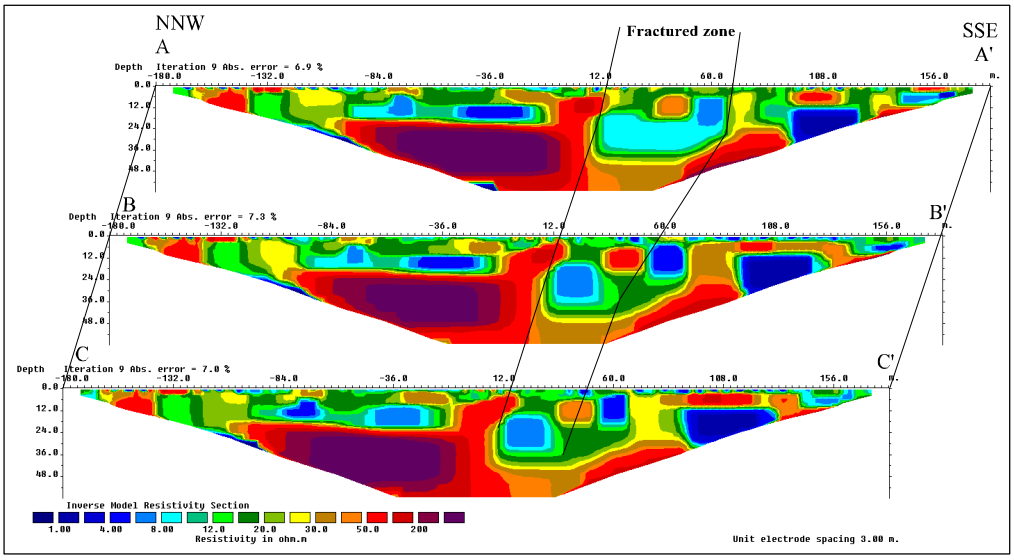

Fig. 6: Inverse resistivity model of the 2-D profiles.

using Taylor and Fleming's method (1988). To interpret the fracture strike graphically, the apparent resistivity for a given square array is plotted against the azimuth of that measurement; the principal fracture strike direction is founded to be perpendicular to the direction of the maximum apparent resistivity (Habberjam, 1972). The apparent anisotropy for square array (λ_a) is given by the ratio of the apparent resistivity measured perpendicular to fracture strike (ρ_{at}) to the apparent resistivity parallel to fracture strike (ρ_{al}) (Darboux-Afouda and Louis 1989), equation 4.

For square array $\lambda_a = \rho_{at}/\rho_{al}$ (4)

RESULTS AND DISCUSSION

Electrical Resistivity Tomography:

The inverse resistivity models of the 2-D profiles illustrate presence of a low resistivity zone to the right from the center of the measured profiles. It has resistivity values vary from 6.0 Ohm.m to 16.0 Ohm.m and it takes NNE-SSW direction (Fig. 6); the low resistivity values of this zone can be attributed to presence of groundwater that saturates this zone; the presence of groundwater tends to reduce the resistivity values of this zone. This zone is located at shallow depths from the ground surface; its depth is approximately 13m. It extends of about 50m along profile A-A' and of about 30m along profiles B-B' and C-C'. Its thickness is about 25m at profiles A-A' and C-C' where it has 27m at profile B-B'. The location of this zone along profile B-B' is selected to carry out the 3-D survey to accurately locate this fractured zone in the compact limestone rocks.

The inverse resistivity model of this 3-D profile is clearly illustrates presence of low resistivity anomaly related to saturated fracture zone that surrounded by high resistivity background related to massive carbonate rocks (Fig. 7). The resistivity values of this zone ranges from 8.0 Ohm.m to 25.0 Ohm.m and it is located at shallow depth (15m) from the ground surface. Its maximum thickness is about 25.9m at its central part; it extends more than 42 m along X-axis. The results obtained from the 3-D model coincide with that obtained from the 2-D profiles over the fractured zone. Based on the previous discussion the best site for drilling new well is recommended over the center of the interpreted fractured zone where it has the maximum thickness (Fig. 8).

Azimuthal Wenner and square array:

The collected data from azimuthal Wenner array indicate a significant variation of apparent resistivity against array azimuth for all a-spacing. The graphical interpretation of these data (Fig. 9A) shows that the maximum apparent resistivity for Wenner array is occurred at N 22.5 degrees for all a-spacing and the dominant fracture strike is parallel to this direction. The calculated effective vertical anisotropy was 1.1, 1.234, 1.364, 1.387 and 1.251for a-spacing 40m, 60m, 80m, 100m and 120m respectively; it changed with depth. The changes in the values of the effective vertical anisotropy can be attributed to slight changes in fracture strike and or changes in fracture amounts with depth.

Also, the data collected from azimuth square array show a significant variation of the apparent resistivity versus the array orientation for all A-spacing. The graphical interpretation of these data (Fig. 9B) shows that the maximum apparent resistivity is founded to be at N 112.5 degrees and the principal fracture strike is oriented at N 22.5 degrees for all A-spacing which are coinciding with the data obtained from the azimuthal Wenner array. The effective vertical anisotropy is 1.342, 1.137 and 1.183 for A-spacing 53.3m, 80m and 106.7m

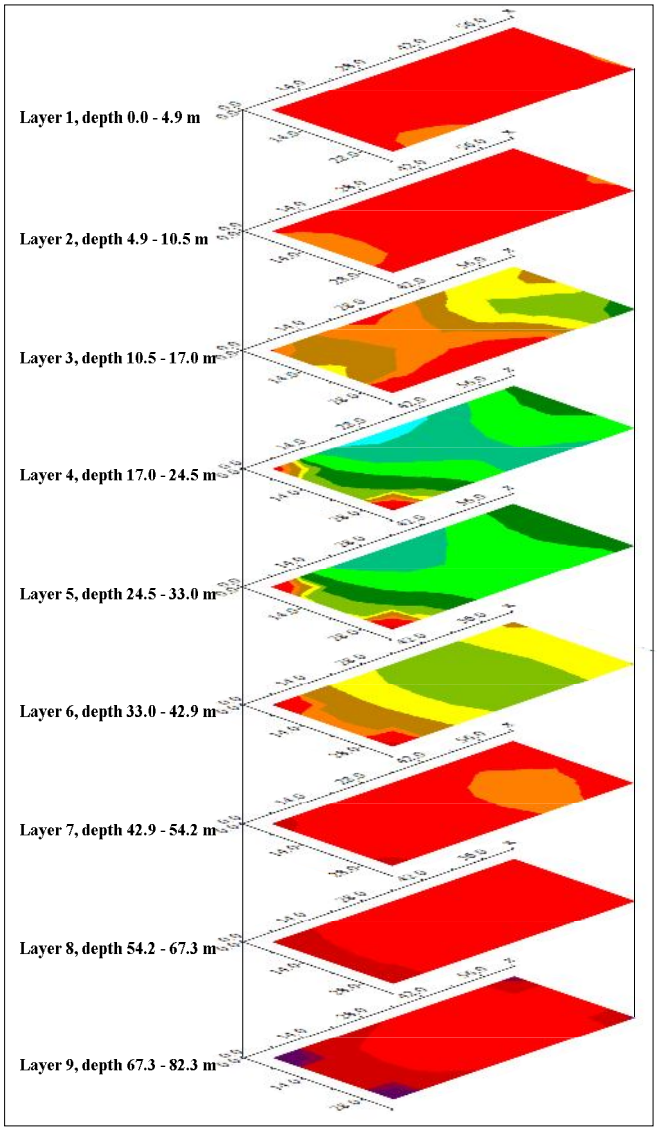

A: Model horizontal slices

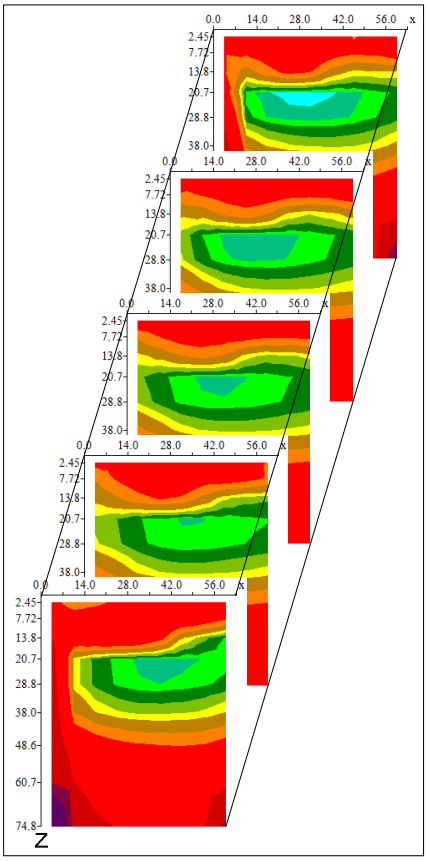

B: Model vertical slices X-Z plane

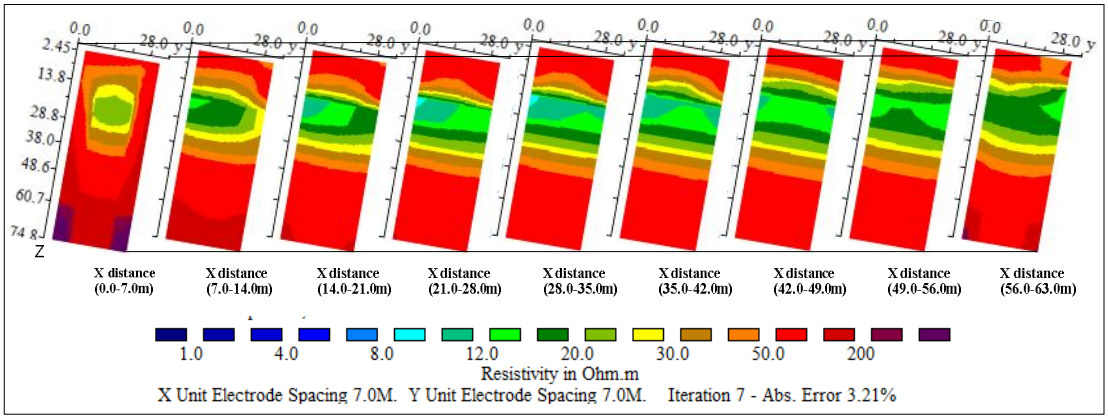

C: Model vertical slices Y-Z plane

Fig. 7: The inverse resistivity model of the 3-D profile.

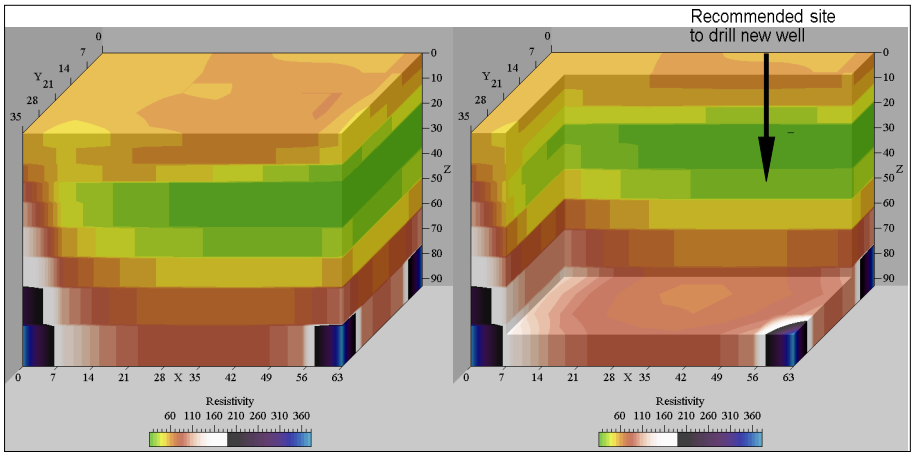

Fig. 8: Block diagram show the best site to drill new well.

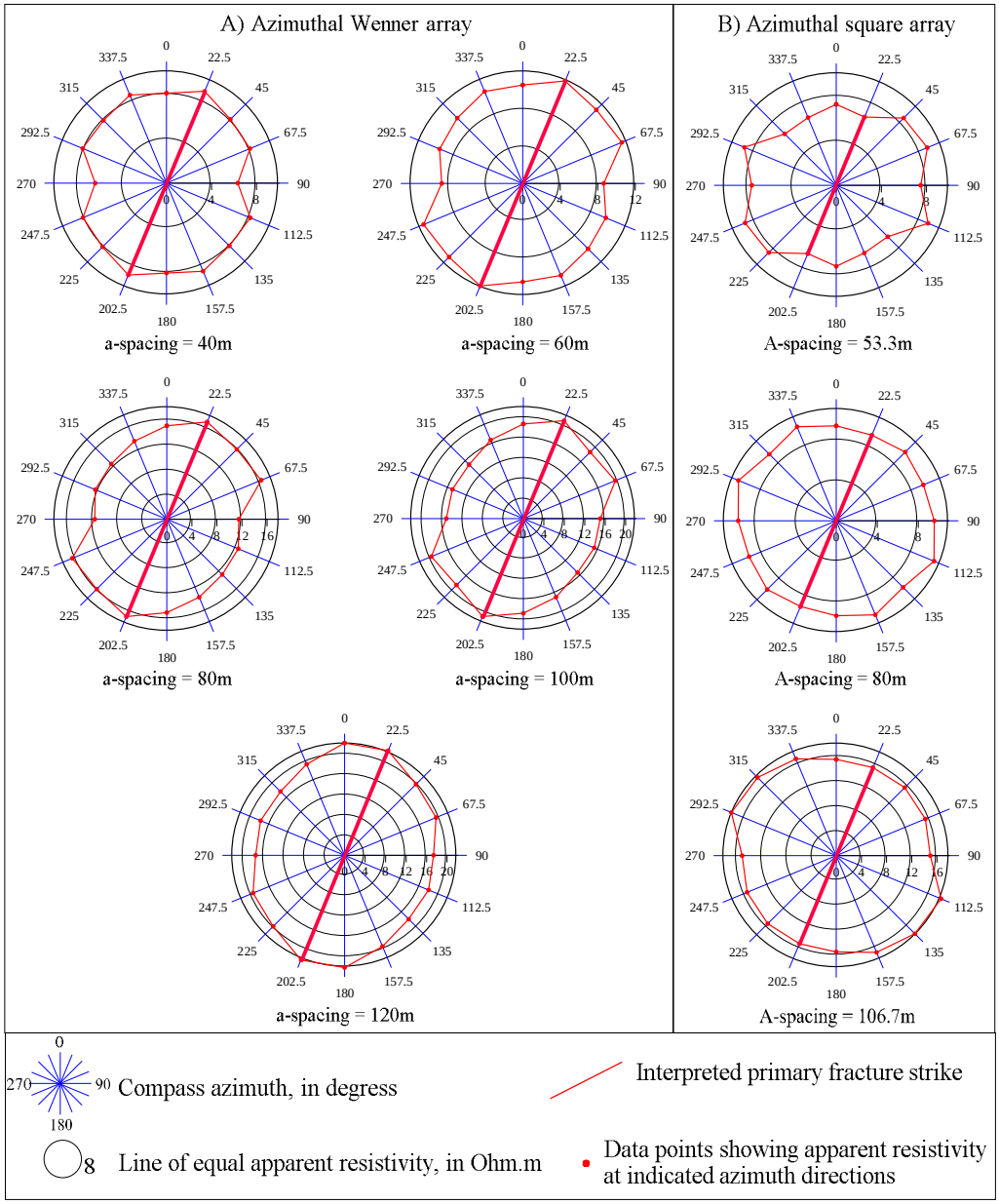

Fig. 9: Apparent resistivity data plotting versus array azimuth.

respectively. The high values of the effective vertical anisotropy obtained from Wenner array indicate that this array is more sensitive to fracture strike than square array at this site due to its good vertical resolution, its high signal strength and its better signal to noise ratio.

Based on the previous discussion, it is clear that the integration between 2-D and 3-D resistivity surveys can accurately led to locate fracture zone in massive carbonate rocks due to hug contrast between the low resistivity fracture zone saturated with groundwater and the high resistivity compact carbonate rocks. Both collinear Wenner and square arrays can be used to determine the fracture orientation and its apparent anisotropy by graphical plotting of the measured apparent resistivity against the azimuth of the array.

CONCLUSION

Groundwater in the arid regions such as El Hassana area represents the unique source of water supplies. The increase demand of water in this arid region needs a lot of efforts to explore new groundwater resources. The inverse resistivity models of the 2-D profiles illustrate presence of a low resistivity zone to the right from their centers. This zone has resistivity values vary from 6.0 Ohm.m to 16.0 Ohm.m and it takes nearly NE-SW direction. It located at shallow depth (13m) and it extended of about 50m along profile A-A' and about 30m along profile C-C'. Its thickness is about 25m at profiles A-A' and C-C' where it has 27m at profile B-B'.

The inverse resistivity model of the 3-D profile illustrates presence of a low resistivity anomaly related to fracture zone surrounded by high resistivity background related to massive carbonate rocks. The resistivity of this zone ranges from 8.0 Ohm.m to 25.0 Ohm.m and its depth is 15 m. The maximum thickness of this zone is about 25.9m and it extends more than 42 m along X-axis. The integration between 2-D and 3-D techniques can be used to accurately locate the low resistivity zone in massive high resistivity carbonate rocks. Based on the results of the ERT techniques the best site for drilling new well is selected over the center of the fracture zone where it has the maximum thickness.

The graphical plotting of the azimuthal Wenner array data indicates a significant variation of apparent resistivity against array azimuth for all a-spacings. The common primary strike of the fractures is found to be oriented at N 22.5 degrees for all a-spacings. The effective vertical anisotropy varies with depth that can be attributed to slight changes in fracture strike and or changes in fractures amount with depth. The graphical plotting of the azimuthal square array data indicates that the principal fracture strike direction is found to be oriented at N 22.5 degrees for all A-spacinngs which are coinciding with the data obtained from the azimuthal Wenner array.

Acknowledgment

Special thanks to Prof. Talaat Ali Abdel Latif and Prof. Mohamed Abass Mabrouk, Emeritus Professors, Geophysical Exploration Dept., Desert Research Center for their advice and review the final manuscript of this work.

REFERENCES

Abou Rayan M., Djebedjian B. and Khaled I. 2001. Water supply and demand and a desalination option for Sinai, Egypt. Desalination 136, 73-81.

Al Abaseiry A.A. 2003. Geoelectrical study to evaluate the factors affecting the groundwater potentialities in El Qusaima area, Northeast Sinai. Egyptian J. Desert Res. 53, (2), 229-241.

Darboux-Afouda R. and Louis P. 1989. Contribution des mesures de l'anisotropic electrique la recherche des aquifres de fracture en milieu cristallin au Benin. Geophysical Prospecting 37, 91-105.

DeGroot-Hedlin C. and Constable S.C. 1990. Occam's inversion to generate smooth, two-dimensional models from magnetotelluric data. Geophysics, 55, 1613-1624.

El Beialy S.Y., Head M.J. and El Atfy H.S. 2010. Palynology of the Mid-Cretaceous Malha and Galala Formations, Gebel El Minshera, North Sinai, Egypt. PALAIOS 25, 517-526.

El Ghazawi M.M. 1989. Hydrogeological studies in Northeast Sinai, Egypt. Ph.D. thesis, Fac. of Sci, El Mansoura Univ. 290p.

El Shamy I.Z. 1992. Towards the water management in Sinai Peninsula. 3rd Conf. Geol. Sinai Develop., Ismailia, 63-70.

El Shazly E.M. 1980. Geologic map of Sinai (Landsat Image, 1972-1975). Academy of Scientific Research and Technology, Egypt, 8p.

GEOTOMO (RES2DINV). 2010. Rapid 2-D Resistivity & IP inversion using the least-squares method. www.geoelectrical.com

GEOTOMO Software. 2010. RES3DINV Ver.2.16. 3D Resistivity and IP Inversion.

Ghorab M.A. 1961. Abnormal stratigraphic features in Ras Gharib oil field. Proceedings of the 3 rd Arab Petrol. Cong., 2: 1-10.

Habberjam G.M. 1972. The effects of anisotropy on square array resistivity measurements. Geophysical Prospecting 20, 249-266.

Habberjam G.M. and Watkins G.E. 1967. The use of a square configuration in resistivity prospecting. Geophysical Prospecting 15, 221-235.

Hammad F.A. 1980. Geomorphological and hydrogeological aspects of Sinai Peninsula. Annals of Geol. Surv. of Egypt 10, 807-817.

Hassan H.F. and Abouelresh M.O. 2013. Characterization of the Campanian-Maastrichtian Sudr Chalk, Gabal El Bruk, North Sinai, Egypt. Faculty of Petroleum and Mining Engineering Journal (FPMEJ) 16-2, 1-16.

Hassanin A.M. 1997. Geological and geomorphological impacts on the water resources in central Sinai, Egypt. Ph.D. thesis, Geol. Dept., Fac. Sci., Ain Shams Univ., P373.

Ioannis F. L., Antonios P. V., Filippos I. L., and Nikolaos T. 2002. The use of geophysical prospecting for imaging the aquifer of Lakka carbonates, Mandoudi Euboea, Greece. Journal of the Balkan Geophysical Socity 5, (3), 97-106.

Issawi B., Francis M.H., Youssef E.A.A., and Osman R.A. 2009. The Phanerozoic Geology of Egypt: A Geodynamic Approach, Second Edition, Special Publication 81, Ministry of Petroleum, The Egyptian Mineral Resources Authority, Cairo, 589 p.

Japan International Cooperation Agency (JICA). 1992. North Sinai groundwater resources study in the A.R.E.. Final Report, 207p.

Lane J.W., Jr., Haeni F.P. and Watson W.M. 1995. Use of a square-array direct-current resistivity method to detect fractures in crystalline bedrock in New Hampshire: Ground Water, V. 33, No. 3, p. 476-485.

Lieblich D.A., Lane J.W., and Haeni F.P. 1991. Results of integrated surface-geophysical studies for shallow subsurface fracture detection at three New Hampshire sites, in Expanded Abstracts with Biographies. SEG 1st Annual International Meeting. Houston, Texas. November 10-14, 1991. Houston, Texas. Society of Exploration Geophysicists. 553-556.

Loke M.H. and Barker R.D. 1996a. Rapid least-squares inversion of apparent resistivity pseudo sections by a quasi-Newton method. Geophysical Prospecting 44, (1), 131–152.

Loke M.H., Acworth I. and Dahlin T. 2003. A comparison of smooth and blocky inversion methods in 2D electrical imaging surveys. Exploration Geophysics, 34, 182-187.

Mahmoud H.H., Barseem M.S., and Youssef A.M. 2015. Application of the two dimensional geoelectric imaging technique to explore shallow groundwater in wadi El Gerafi basin, Eastern Central Sinai – Egypt. Arab J Geosci 8, (6), 3589–3601.

Massoud U. 2005. Geophysical studies for groundwater exploration in El Bruk area, North Central Sinai, Egypt. Ph.D. Thesis, Fac. of Science, Minufiya Univ., 130p.

Metwaly M. and AlFouzan F. 2013. Application of 2-D geoelectrical resistivity tomography for subsurface cavity detection in the eastern part of Saudi Arabia. J. of Geoscience Frontiers 4, 469-476.

Moustafa A.R. and Khalil M.H. 1989. North Sinai structures and tectonic evolution. Middle East Research Center, Ain Shams Univ., Earth Sci., Ser. 3, 215-231.

Rabeh T.T. and Miranda J.M. 2007. Evaluating the subsurface structures due to the Syrian Arc tectonics at El Hasana area, Sinai Peninsula, Egypt. Acta Geod. Geoph. Hung. 42, (4), 465-478.

Ritzi R.W. and Andolsek R.H. 1992. Relation between anisotropic transmissivity and azimuthal resistivity surveys in shallow fractured carbonate flow systems. Ground Water 30, (5), 774-780.

Sehli A.S. 1990. Contribution of electrical prospecting to the geophysical study of discontinuous media, in International symposium on applications of geophysics to water prospecting in arid and semi-arid areas. Paris, France.

Shata A.A. 1956. Structural development of the Sinai Peninsula, Egypt: Bull. Inst. Desert, Egypt 6, (2), 117-157.

Shata A.A. 1960. The geology and geomorphology of El Qusaima area. Bull. Soc. Geograph. Egypt, 95-146.

Sultan S.A., Sabet, H.S., and Gaweish W.R. 2015. Integrated geophysical interpretation for delineating the structural elements and groundwater aquifers at central part of Sinai Peninsula, Egypt. J. of African Earth Sciences 105, 93-106.

Tanguy R., Alain D., Serge B., Olivier K.,Vincent H., and Frédéric N. 2011. Assessing the contribution of electrical resistivity tomography (ERT) and self-potential (SP) methods for a water well drilling program in fractured/karstified limestones. Journal of Applied Geophysics 75, 42–53.

Tassy A., Maxwell M., Borgomano J., Arfib B., Fournier F., Gilli E., and Guglielmi Y. 2014. Electrical resistivity tomography (ERT) of a coastal carbonate aquifer (Port-Miou, SE France). Environmental Earth Sciences 71, (2), 601-608.

Taylor R.W. and Fleming A.H. 1988. Characterizing jointed systems by azimuthal resistivity surveys. Ground Water 26, (4), 464-474.

White R.M.S., Collins S., Denne R., Hee R. and Brown P. 2001. A new survey design for 3D IP modelling at Copper hill. Exploration Geophysics, 32, 152-155.

Yadav G.S. and Singh S.K. 2007. Integrated resistivity surveys for delineation of fractures for ground water exploration in hard rock areas. Journal of Applied Geophysics 62, (3), 301–312.